J Mol Model (2011) 17:1847–1854
DOI 10.1007/s00894-010-0890-6

ORIGINAL PAPER

A computational study of CYP3A4 mediated drug interaction profiles for anti-HIV drugs

Jayakanthan Mannu · Pranitha Jenardhanan · Premendu P. Mathur

Received: 9 July 2010 / Accepted: 22 October 2010 / Published online: 16 November 2010

Abstract Molecular docking is a reliable method with which to identify the binding conformations of substrates, inducers and inhibitors of cytochrome P450 (CYP) enzymes. We used the docking method to explore possible binding modes of an entry inhibitor (maraviroc) and non-nucleoside reverse transcriptase inhibitors (delavirdine, efavirenz and etravirine) to cytochrome P450 3A4 (CYP3A4). In addition, docking results were compared with the binding conformations of HIV protease drugs to infer the binding site residues and potential drug–drug interaction profiles for combination therapy in the treatment of AIDS. We observed that efavirenz and etravirine induce metabolism of co-administered drugs by binding to a unique position in the active site of CYP3A4. Dosage adjustment is required for delavirdine and maraviroc when combined with HIV protease drugs. The present results are in good agreement with experimental data from drug interaction profiles. The information provided in this paper will be helpful in furthering our understanding the functions of CYP3A4, and could aid in the design of new drugs that would be metabolized easily without having any drug–drug interaction profile.

Keywords Binding conformation · CYP3A4 · Drug–drug interaction · Docking · Entry inhibitor · NNRTI

J. Mannu · P. Jenardhanan · P. P. Mathur (✉)
Centre of Excellence in Bioinformatics, School of Life Sciences,
Pondicherry University,
Pondicherry 605014, India
e-mail: ppmathur@gmail.com

P. P. Mathur
e-mail: ppmathur.bic@pondiuni.edu.in

Introduction

Highly active antiretroviral therapy (HAART), or combination therapy, is the recommended treatment to control the reproduction of the HIV virus and to slow down the progression of HIV-related diseases [1, 2]. HAART combines three or more anti-HIV drugs in a daily regimen. Cytochrome P450 3A4 (CYP3A4) is the major isozyme responsible for metabolism of many marketed drugs [3]. The three classes of anti-HIV drugs that are metabolized primarily by CYP3A4 are: (1) non-nucleoside reverse transcriptase inhibitors (NNRTIs: delavirdine, efavirenz and etravirine); (2) entry inhibitors (maraviroc); and (3) protease inhibitors [ritonavir (RTV), amprenavir (APV), tipranavir (TPV), indinavir (IDV), saquinavir (SQV), nelfinavir (NFV), lopinavir (LPV), fosamprenavir (FOS-APV), darunavir and atazanavir (ATV)] [4]. In patients receiving these drugs in combination for HAART, adverse drug–drug interactions for the same metabolizing enzyme CYP3A4 are possible. These could lead to unwanted and life-threatening effects by elevating blood levels of the competing drugs [5]. Hence, for more effective and less toxic treatment it is important that co-administered anti-HIV drugs should have different modes of binding to CYP3A4 for metabolic clearance.

In recent years, molecular docking methods have been very useful in elucidating the binding properties of ligands to the active site of cytochrome P450 [6–9]. In previous studies from our laboratory, we showed that TPV, NFV, LPV, and ATV differ in their binding conformations, whereas RTV, APV, IDV, SQV, FOS-APV, and darunavir share the same binding mode for metabolic clearance through CYP3A4 [10]. The amino acids Arg212, Arg105, Arg106, Glu374, Ser119, Ala370, and Arg372 were identified as key residues in this metabolism. In the present

study, we carried out molecular docking studies to investigate the binding modes with CYP3A4 of NNRTIs and an entry inhibitor in order to infer drug–drug interaction profiles of the competing drugs used in combination or salvage therapy.

Materials and methods

Molecular structures and optimization

The human microsomal cytochrome P450 3A4 structure (PDB Code: 1TQN) was obtained from Protein Data Bank (http://www.rcsb.org/pdb) [11]. This structure was determined by X-ray crystallography at 2.05 Å resolution [12]. The two classes of drug molecules used in this work include NNRTIs and an entry inhibitor. These drugs [delavirdine (CID: 5625), efavirenz (CID: 64139), etravirine (CID: 193962) and maraviroc (CID: 3002977)] were obtained from the NCBI-PubChem Compound database (http://pubchem.ncbi.nlm.nih.gov/). The two dimensional structures of these compounds are shown in Fig. 1. The structure geometries were subsequently optimized using the Steepest Descent method followed by Conjugate Gradient in 2,000 steps using Accelrys Discovery Studio (Version 2.1, Accelrys Software, http://accelrys.com/). Optimization was carried out by applying the CHARMm force field.

Molecular docking

Docking simulations on CYP3A4 were carried out using the AutoDock 4.0 software package [13]. The components of the program include AutoTors, AutoGrid and AutoDock. AutoTors defines which bonds in the ligand are rotatable. Based on the size of the drug molecules used here, the number of rotatable bonds was varied in the range of three to nine, and bonds were allowed to rotate freely. AutoGrid was used to generate grid maps for each ligand. AutoGrid pre-calculates three-dimensional grid maps, one for each type of atom present in the ligand, and stores the interaction energy based on a macromolecular target using the AMBER force field. AutoDock 4.0 was used for the task of docking. The graphical user interface 'AutoDock Tools' was used to prepare, run, and analyze the docking simulations.

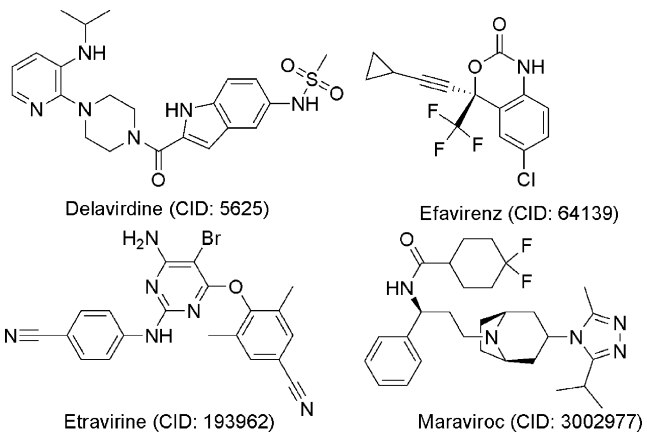

Fig. 1 Chemical structures of three non-nucleoside reverse transcriptase inhibitors (NNRTIs) and one entry inhibitor used in this study

Preparation of protein and ligands

The CYP3A4 protein structure was prepared by assigning Kollman united-atom charges, solvation parameters and polar hydrogens, and removing water molecules. Since the drugs are not peptides, Gasteiger charge was added and non-polar hydrogens merged. The rigid roots of each drug were defined automatically and amide bonds were made non-rotatable.

CYP3A4 cavity size and grid generation

The most interesting features of the CYP3A4 structures are the size and shape of the active site cavity [14]. This cavity is much larger near the heme iron. Two different volumes of active site cavity are reported in the literature, i.e., 1,386 $Å^3$ and 520 $Å^3$ [12, 15]. These large binding site cavities allow this enzyme to accommodate substrates of diverse size. The size would also indicate that more than one substrate can bind the enzyme simultaneously [16–18]. The grid box was fixed at the center of the heme moiety. The box size was normally set at 60 × 60 × 60 Å in the x, y and z axes. AutoGrid was used to produce grid maps. The spacing between grid points was 0.375 Å.

Docking search method

The conformer search method used was the Lamarckian genetic algorithm (LGA). LGA is a combination of a genetic algorithm with a local search method to perform energy minimization. We chose 50 runs of LGA (default is ten conformers) for each drug molecule. This method is used to produce binding energy as a scoring function. Williams et al. [15] have determined three crystal structures of CYP3A4—unliganded, bound to the inhibitor metyrapone, and bound to substrate progesterone—to investigate whether conformational movement is a necessary prerequisite for ligand binding. Contrary to their expectations, binding of metyrapone and progesterone to CYP3A4 revealed essentially no conformational changes in the protein. In addition, superimposition of all the available PDB crystal structures of CYP3A4 shows that very little conformational change occurs in the protein conformation. Hence we kept the target protein structure rigid and the

drugs flexible during the search process. The number of individuals in each population was set at 150. The maximum number of energy evaluations was set at 250,000. The maximum number of generations was set at 1,000. The maximum number of top individuals that automatically survived was set at 1. The rates of gene mutation and crossover were set at 0.02 and 0.8, respectively.

Hardware and software

The calculation of AutoGrid and AutoDock were performed on an Intel Pentium PD-925 CPU @ 3.0 GHz of HCL infosystem origin, with 2 GB DDR RAM. AutoDock 4.0 was compiled and run under the Microsoft Windows XP operating system.

Results and discussion

CYP3A4 is a complex heme-containing enzyme involved in the metabolism of more than 50% of marketed drugs. It is the isozyme most implicated in drug–drug interaction profiles [19]. A better understanding of molecular interactions between CYP3A4 and drugs would lead to helpful insights for the development of new medications. Here, we present the molecular interactions of NNRTIs and an entry inhibitor with CYP3A4 using an in silico docking study; the results are also compared with our previous docking results of HIV-1 protease inhibitors [10]. As revealed by site-directed mutagenesis and X-ray crystallography studies, the most important amino acids involved in the active site of CYP3A4 are Ser119, Ile301, Phe304, Ala305, Ile369, Ala370 and Glu374 [12, 15, 20–22]. The Protein Data Bank has crystal structures of human CYP3A4 in the unliganded form (1TQN and 1W0E), bound to inhibitors (1W0G, 2J0D and 2V0M) and bound to substrate (1W0F) at different resolutions. The protein structure with PDB ID:1TQN has a high resolution of 2.05 Å as compared to other crystal structures. Superimposition of all the above crystal structures using the 'align structures' module in the Accelrys Discovery Studio shows that the protein conformation of liganded complexes is very similar to the ligand-free structure exemplified by 1TQN [main chain RMSD is 0.731 Å (1W0E), 0.621 Å (1W0F), 0.716 Å (1W0G), 0.939 Å (2J0D) and 1.188 Å (2V0M)]. Hence, to select the most suitable conformation for our docking studies, a high resolution crystal structure was used as a criteria and 1TQN was selected. The first step in the docking study is structure optimization, during which we carried out energy minimization by Steepest Descent followed by the Conjugate Gradient method. The optimization values are given in Table 1. The 50 docked conformations of each drug were clustered based on a root mean squares deviation (RMSD) tolerance of 2.0 Å. Structurally similar clusters were ranked in order of increasing binding energies and the values are given in Table 2. The best docked conformation was selected as the one which has the lowest binding free energy from the top ranked clusters of conformations. The docked conformations of each of the NNRTIs and the entry inhibitor with CYP3A4 are discussed below.

Delavirdine

The NNRTI delavirdine is a bisheteroarylpiperazine derivative that is extensively metabolized by CYP3A4 [23]. The docked simulation of delavirdine produced 17 clusters of conformers in the RMSD tolerance of 2.0 Å from 50 runs of LGA (Table 2). In analyzing the number of conformations in each cluster, first and second have 9 and 16 conformations, respectively. Generally, producing a large number of conformations in a single cluster indicates a high frequency of occurrence of the same pose in the binding pocket. Hence, we selected the complex conformation of least binding energy from the second cluster of conformers in order to analyze the binding mode of the drug. The binding energy of the selected conformation was -9.93 kcalmol^{-1} (Table 3).

Table 1 Minimization energy values of anti-HIV drugs. *NNRTI* Non-nucleoside reverse transcriptase inhibitor, *Int PE* initial potential energy, *PE* potential energy, *VdwE* van der Waals energy; *EE* electrostatic energy

Anti-HIV drug	Energy levels after Steepest Descent in 2,000 steps (kcal/mol)				Energy levels after Conjugate Gradient in 2,000 steps (kcal/mol)			
	Int PE	PE	VdwE	EE	Int PE	PE	VdwE	EE
NNRTI								
Delavirdine	23.79185	-3.01882	-2.39672	-24.29452	-3.01866	-4.76999	-3.38547	-24.33664
Efavirenz	3.60817	-6.63003	2.51943	-29.77647	-6.62998	-7.06713	3.04281	-30.92578
Etravirine	-12.09436	-29.61190	1.75978	-45.49706	-29.61183	-30.23357	1.17141	-45.80035
Entry inhibitor—CCR5 co-receptor antagonist								
Maraviroc	49.85536	37.54393	-18.38037	-13.22489	37.54397	34.52613	-20.99919	-14.35135

Table 2 Summary of conformational clusters found out of 50 runs using a root mean squares deviation (RMSD) tolerance of 2.0 Å

Anti-HIV drug	Number of cluster	Cluster rank	Lowest binding energy (kcal/mol)	Mean binding energy (kcal/mol)	Runs in cluster
NNRTI					
Delavirdine	17	1	-10.45	-8.77	9
		2	-9.93	-8.61	16
		3	-9.39	-8.30	7
		4	-9.30	-9.30	1
		5	-9.00	-8.45	4
		6	-8.65	-8.65	1
		7	-8.42	-8.42	1
		8	-6.60	-6.60	1
		9	-6.49	-6.49	1
		10	-6.37	-6.37	1
		11	-5.82	-5.82	1
		12	-4.99	-4.57	2
		13	-4.86	-4.86	1
		14	-4.33	-4.33	1
		15	-3.97	-3.97	1
		16	-3.55	-3.55	1
		17	-3.13	-3.13	1
Efavirenz	4	1	-6.75	-6.71	38
		2	-6.62	-6.62	1
		3	-6.36	-6.34	5
		4	-6.25	-6.23	6
Etravirine	10	1	-9.11	-8.54	26
		2	-8.66	-7.93	3
		3	-8.61	-8.28	5
		4	-8.52	-8.44	3
		5	-8.26	-8.26	1
		6	-8.15	-7.99	6
		7	-8.12	-8.00	3
		8	-7.75	-7.75	1
		9	-7.47	-7.47	1
		10	-6.69	-6.69	1
Entry inhibitor—CCR5 co-receptor antagonist					
Maraviroc	18	1	-12.03	-9.09	9
		2	-10.13	-7.91	7
		3	-9.18	-6.22	7
		4	-8.84	-8.02	5
		5	-8.64	-7.03	2
		6	-8.62	-8.62	1
		7	-8.43	-7.12	2
		8	-8.10	-6.75	2
		9	-8.06	-6.53	3
		10	-7.82	-6.71	3
		11	-7.48	-7.48	1
		12	-7.25	-7.02	2
		13	-6.77	-6.77	1
		14	-6.48	-6.48	1
		15	-5.44	-5.44	1
		16	-5.30	-5.30	1
		17	-3.42	-3.42	1
		18	-1.52	-1.52	1

The docked complex of delavirdine was involved in the formation of a single hydrogen bond in which the backbone oxygen atom of Ser119 acts as a hydrogen bond acceptor and a hydrogen of the drug as the donor atom (Fig. 2a). The bond distance between these two atoms was 1.824 Å. The residues Phe108, Arg212, Phe215, Ala305, Ile369, Ala370, Met371, Glu374 and Hem508 were involved in van der Waals interactions in the scaling factor of 1.00 Å. The unique nature of the CYP3A4 enzyme is the occurrence of drug–drug interactions when drugs compete for metabolism. Delavirdine is an inhibitor of CYP3A4 enzyme and inhibits the metabolism of HIV protease drugs during combination therapy, leading to increased levels of these drugs in the plasma [23–26]. Experimental results, which are reproduced by our docking method, show that delavirdine adopts diverse conformations to inhibit CYP3A4-mediated metabolism of protease-based drugs, possibly by sharing the same binding site residues, as observed from the formation of a large number of clusters with a single conformation in each cluster (Table 2).

Efavirenz

The NNRTI efavirenz is usually recommended as an initial therapy with potential antiviral activity against HIV strains [27]. This drug is an effective inducer of CYP3A4 enzyme, thereby reducing exposure of the plasma to HIV protease drugs in combination therapy [28–30]. Hence, analyzing docked conformations of efavirenz will yield valuable information on drug–drug interactions for HIV protease drugs. The 50 runs of docking simulation of efavirenz to CYP3A4 resulted in the formation of four cluster conformations (Table 2). The conformations of the first ranked cluster were highly favored statistically and were repeated 38 times with a high frequency of occurrence, indicating increased specificity of this binding conformation of efavirenz into CYP3A4. The lowest binding energy of the first ranked cluster conformation was -6.75 kcalmol^{-1}. The docking pose of efavirenz produced multiple hydrogen bonds with the residue of Ser119 (Fig. 2b). In addition, Arg105, Phe108, Arg212, Arg372, Leu373, Glu374, Phe304, Ala305 and Hem508 participated in van der Waals interactions to further stabilize binding of the drug. Assessing the docked conformations of all HIV-protease drugs [10] shows that efavirenz differs in its binding mode in terms of hydrogen bond formation, with the exception of atazanavir since both drugs use Ser119 for interaction. Thus, we conclude that efavirenz can bind to a unique position in the active site of CYP3A4 and induces the metabolism of other antiviral drugs. This conclusion is consistent with experimental data on HIV protease drug metabolism [28–30].

Table 3 Molecular interactions of anti-HIV drugs with cytochrome P450 3A4 ((CYP3A4)

Anti-HIV drug	Hydrogen bond donor	Hydrogen bond acceptor	Hydrogen bond length (Å)	vdW interaction residues (scaling factor=1.00 Å)	Binding free energy (kcal/mol)	Docking energy (kcal/mol)
NNRTI						
Delavirdine	DRUG::H42	CYP:A:SER119:OG	1.824	PHE108, ARG212, PHE215, ALA305, ILE369, ALA370, MET371, GLU374, HEM508	-9.93	-11.58
Efavirenz	DRUG::H28 CYP:A:SER119:HG	CYP:A:SER119:OG DRUG::O6	2.036 2.226	ARG105, PHE108, ARG212, PHE304, ALA305, ARG372, LEU373, GLU374, HEM508	-6.25	-7.45
Etravirine	DRUG::H37	CYP:A:ARG372:O	1.968	PHE57, ARG105, PHE108, SER119, ARG212, ILE369, ALA370, MET371, GLU374, HEM508	-9.11	-10.83
Entry inhibitor—CCR5 co-receptor antagonist						
Maraviroc	CYP:A:ARG212: HH22	DRUG::O3	1.96	PHE57, ARG105, ARG106, PHE108, SER119, PHE213, PHE215, PHE304, ALA305, MET371, ARG372, GLU374, HEM508	-12.03	-14.08

Etravirine

Etravirine is a new drug in the NNRTI family approved by US-FDA for the treatment of HIV infection. The molecular docking study of etravirine to CYP3A4 results in the formation of ten clusters, of which the first ranked cluster contains 26 conformations (Table 2). We found that both etravirine and efavirenz produced a greater number of conformations in the first ranked cluster with an RMSD of 2.0 Å from 50 LGA runs, which shows the possibility of producing more specific binding conformations to the CYP3A4 enzyme. The amino acid residue Arg372 was involved in hydrogen bond formation, whereas Phe57, Arg105, Phe108, Ser119, Arg212, Ile369, Ala370, Met371, Glu374 and Hem508 mediated van der Waals forces to the etravirine drug (Fig. 3a). Comparing the binding site residues of etravirine with HIV protease drugs [10] revealed that, with the exception of nelfinavir, they differ in their binding modes in terms of hydrogen bond formation. One possible reason for this is that etravirine is a highly flexible di-aryl pyrimidine compound, which enables more favorable binding with CYP3A4. Since etravirine and efavirenz are inducers of the CYP3A4 enzyme, we also conclude that these drugs bind to unique positions in the active site and mediate the metabolism of other antiviral drugs. This observation is consistent with experimental data showing

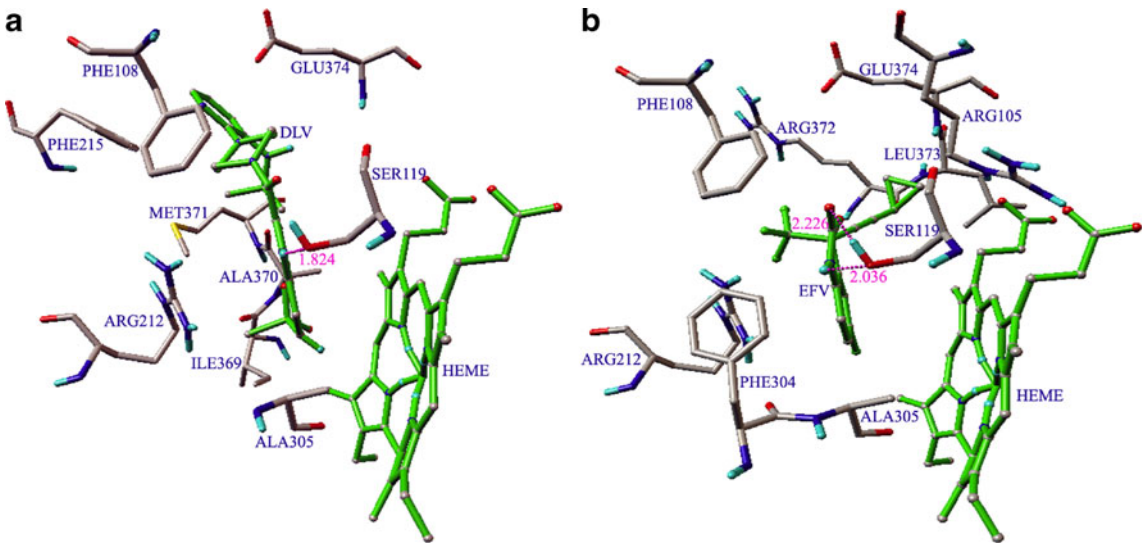

Fig. 2 The docked poses of (**a**) delavirdine (DLV) and (**b**) efavirenz (EFV) inside the active site of cytochrome P450 3A4 (CYP3A4). The conformations are shown in ball and stick representation. The binding site residues are colored by atom type: *gray* carbon, *red* oxygen, *blue* nitrogen, *cyan* hydrogen, *yellow* sulfur. The sticks of the ligands and heme are colored in *green*. The hydrogen bond is depicted as a *pink line* together with its bond length

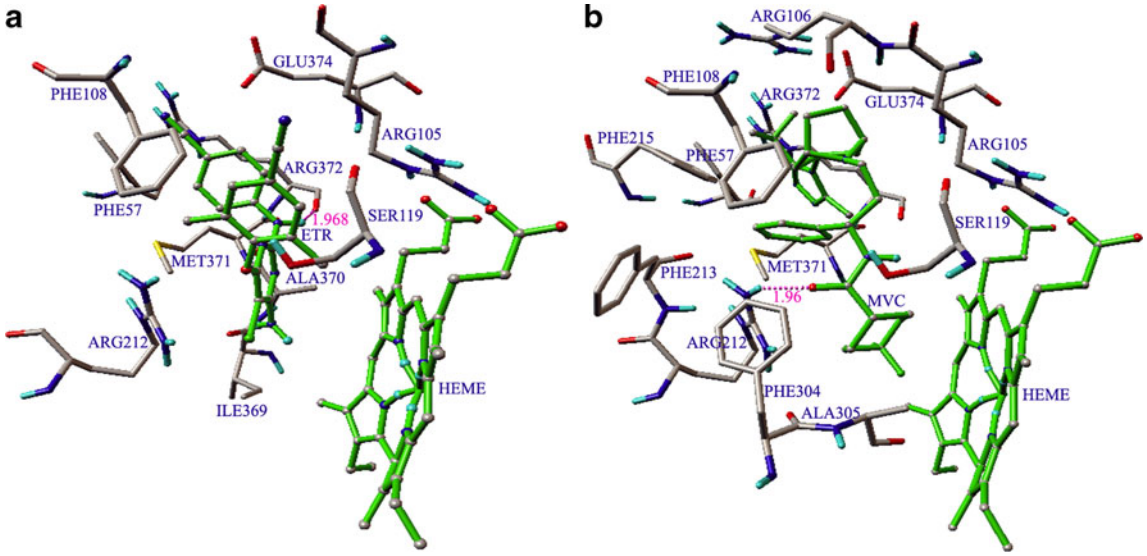

Fig. 3 The docked poses of (**a**) etravirine (ETR) and (**b**) maraviroc (MVC) inside the active site of CYP3A4

that etravirine lacks a significant drug interaction profile and can be used as a suitable drug in combination therapy [4, 31–33]. The binding free energy and docking energy calculated for etravirine with CYP3A4 were −9.11 and −10.83 kcal mol^{-1}, respectively.

Maraviroc

Maraviroc, a potent CCR5 co-receptor antagonist, is a member of new class of antiretroviral drugs called entry inhibitors. This drug is metabolized extensively by CYP3A4 and dosage adjustment is required when administered in combination with CYP3A4 inhibitors or inducers as a concomitant drug [34]. The dosage of maraviroc should be reduced when combined with HIV protease drugs except tipranavir, whereas the dose should be increased when combined with etravirine or efavirenz [4, 35, 36]. The number of cluster conformers produced in the docking of maraviroc to CYP3A4 was 18, with fewer conformations in each cluster (Table 2), confirming that maraviroc should bind to CYP3A4 each time with a different pose. This would result in utilizing the same binding site residues for CYP3A4-mediated metabolic interactions of concomitant drugs, leading to increased levels of maraviroc in the plasma. The calculated binding free energy of the docked CYP3A4–maraviroc complex was −12.03 kcal mol^{-1}. The side chain hydrogen atom of Arg212 acts as a hydrogen bond donor, forming a single bond with the oxygen atom of the drug (Table 3). In addition, Phe57, Arg105, Arg106, Phe108, Ser119, Phe213, Phe215, Phe304, Ala305, Met371, Arg372, Glu374 and Hem508 contribute to van der Waals interactions to maraviroc at a scaling factor of 1.00 Å (Fig. 3b). Upon detailed assessment of binding site residues, maximum numbers of phenylalanine and arginine were involved in the interactions. The binding conformations of maraviroc, ritonavir, amprenavir, indinavir, saquinavir and darunavir share the same binding site residue (i.e., Arg212) involved in hydrogen bond formation for metabolic interactions [10], which is consistent with experimental data showing elevated plasma concentrations of maraviroc [4]. On the other hand, maraviroc differs in its binding mode from efavirenz and etravirine for CYP3A4 interactions, thus explaining the increased metabolism of this drug [35].

Conclusions

Many physiological and pathological factors can alter the metabolism of drugs, and abrupt metabolism of concomitant medications is of much concern. However, metabolic drug–drug interaction studies are being used effectively to explore the possible effects of investigational agents on the metabolism of drugs already on the market as well as the effects of such commercial drugs on the metabolism of investigational agents. Although various in vitro and in vivo techniques are used to study metabolic drug–drug interactions, computational molecular docking studies also offer equally useful information for predicting such interactions. In this paper, we were concerned with the interactions of an entry inhibitor and NNRTIs with CYP3A4, and we revealed how these compounds bind to CYP3A4 for metabolic clearance. The docking results show that efavirenz and etravirine can induce the metabolism of concomitant drugs by binding to unique positions in the active site of the CYP3A4 isozyme. The large numbers of cluster conformations produced by docking of delavirdine and maraviroc shows the broad specificity of these

compounds to bind to the same position in the active site of CYP3A4. We infer that delavirdine and maraviroc can alter the concentration of HIV protease drugs in the plasma by interfering with same binding site residues in CYP3A4.

Based on these interaction studies, we observed that Ser119, Arg212 and Arg372 are the major drug binding residues in CYP3A4 for metabolic clearance. The precise binding residues revealed in this study will be constructive in developing new drugs with better metabolic insights.

Acknowledgments P.P. Mathur acknowledges receipt of financial support from the Department of Biotechnology (DBT), and the Department of Information Technology (DIT), Government of India, New Delhi, India.

References

1. Sterne JA, Hernan MA, Ledergerber B, Tilling K, Weber R, Sendi P, Rickenbach M, Robins JM, Egger M (2005) Long-term effectiveness of potent antiretroviral therapy in preventing aids and death: a prospective cohort study. Lancet 366:378–384. doi:10.1016/S0140-6736(05)67022-5
2. Gange SJ, Barron Y, Greenblatt RM, Anastos K, Minkoff H, Young M, Kovacs A, Cohen M, Meyer WA 3rd, Munoz A (2002) Effectiveness of highly active antiretroviral therapy among hiv-1 infected women. J Epidemiol Commun Health 56:153–159. doi:10.1136/jech.56.2.153
3. Sheweita SA (2000) Drug-metabolizing enzymes: mechanisms and functions. Curr Drug Metab 1:107–132. doi:10.2174/1389200003339117
4. Brown KC, Paul S, Kashuba ADM (2009) Drug interactions with new and investigational antiretrovirals. Clin Pharmacokinet 48:211–241. doi:10.2165/00003088-200948040-00001
5. Tanaka E (1998) Clinically important pharmacokinetic drug-drug interactions: role of cytochrome p450 enzymes. J Clin Pharm Ther 23:403–416. doi:10.1046/j.1365-2710.1998.00086x
6. Kjellander B, Masimirembwa CM, Zamora I (2007) Exploration of enzyme-ligand interactions in cyp2d6 and 3a4 homology models and crystal structures using a novel computational approach. J Chem Inf Model 47:1234–1247. doi:10.1021/ci600561v
7. Oda A, Yamaotsu N, Hirono S (2004) Studies of binding modes of (s)-mephenytoin to wild types and mutants of cytochrome P450 2 C19 and 2 C9 using homology modeling and computational docking. Pharm Res 21:2270–2278. doi:10.1007/s11095-004-7680-8
8. Ito Y, Kondo H, Goldfarb PS, Lewis DF (2008) Analysis of cyp2d6 substrate interactions by computational methods. J Mol Graph Model 26:947–956. doi:10.1016/j.jmgm.2007.07.004
9. Yao Y, Han WW, Zhou YH, Li ZS, Li Q, Chen XY, Zhong DF (2009) The metabolism of cyp2c9 and cyp2c19 for gliclazide by homology modeling and docking study. Eur J Med Chem 44:854–861. doi:10.1016/j.ejmech.2008.04.015
10. Jayakanthan M, Chandrasekar S, Muthukumaran J, Mathur PP (2010) Analysis of cyp3a4-hiv-1 protease drugs interactions by computational methods for highly active antiretroviral therapy in hiv/aids. J Mol Graph Model 28:455–463. doi:10.1016/j.jmgm.2009.10.005
11. Berman H, Henrick K, Nakamura H, Markley JL (2007) The worldwide protein data bank (wwpdb): ensuring a single, uniform archive of pdb data. Nucleic Acids Res 35:D301–303. doi:10.1093/nar/gkl971
12. Yano JK, Wester MR, Schoch GA, Griffin KJ, Stout CD, Johnson EF (2004) The structure of human microsomal cytochrome P450 3A4 determined by X-ray crystallography to 2.05-Å resolution. J Biol Chem 279:38091–38094. doi:10.1074/jbc.C400293200
13. Morris GM, Goodsell DS, Halliday RS, Huey R, Hart WE, Belew RK, Olson AJ (1998) Automated docking using a Lamarckian genetic algorithm and an empirical binding free energy function. J Comput Chem 19:1639–1662. doi:10.1002/(SICI)1096-987X(19981115)19:14<1639::AID-JCC10>3.0.CO;2-B
14. Scott EE, Halpert JR (2005) Structures of cytochrome p450 3a4. Trends Biochem Sci 30:5–7. doi:10.1016/j.tibs.2004.11.004
15. Williams PA, Cosme J, Vinkovic DM, Ward A, Angove HC, Day PJ, Vonrhein C, Tickle IJ, Jhoti H (2004) Crystal structures of human cytochrome p450 3a4 bound to metyrapone and progesterone. Science 305:683–686. doi:10.1126/science.1099736
16. Kapelyukh Y, Paine MJ, Marechal JD, Sutcliffe MJI, Wolf CR, Roberts GCK (2008) Multiple substrate binding by cytochrome p450 3a4: estimation of the number of bound substrate molecules. Drug Metab Dispos 36:2136–2144. doi:10.1124/dmd.108.021733
17. Korzekwa KR, Krishnamachary N, Shou M, Ogai A, Parise RA, Rettie AE, Gonzalez FJ, Tracy TS (1998) Evaluation of atypical cytochrome p450 kinetics with two-substrate models: evidence that multiple substrates can simultaneously bind to cytochrome p450 active sites. Biochemistry 37:4137–4147. doi:10.1021/bi9715627
18. Shou M, Grogan J, Mancewicz JA, Krausz KW, Gonzalez FJ, Gelboin HV, Korzekwa KR (1994) Activation of CYP3A4: evidence for the simultaneous binding of two substrates in a cytochrome p450 active site. Biochemistry 33:6450–6455. doi:10.1021/bi00187a009
19. Gibbs MA, Hosea NA (2003) Factors affecting the clinical development of cytochrome p450 3a substrates. Clin Pharmacokinet 42:969–984
20. Fowler SM, Taylor JM, Friedberg T, Wolf CR, Riley RJ (2002) CYP3A4 active site volume modification by mutagenesis of leucine 211. Drug Metab Dispos 30:452–456. doi:10.1124/dmd.30.4.452
21. Fowler SM, Riley RJ, Pritchard MP, Sutcliffe MJ, Friedberg T, Wolf CR (2000) Amino acid 305 determines catalytic center accessibility in CYP3A4. Biochemistry 39:4406–4414. doi:10.1021/bi992372u
22. Roussel F, Khan KK, Halpert JR (2000) The importance of SRS-1 residues in catalytic specificity of human cytochrome P450 3A4. Arch Biochem Biophys 374:269–278. doi:10.1006/abbi.1999.1599
23. Tran JQ, Gerber JG, Kerr BM (2001) Delavirdine: clinical pharmacokinetics and drug interactions. Clin Pharmacokinet 40:207–226. doi:10.1006/abbi.1999.1599
24. Harris M, Alexander C, O'Shaughnessy M, Montaner JSG (2002) Delavirdine increases drug exposure of ritonavir-boosted protease inhibitors. AIDS 16:798–799
25. Scott LJ, Perry CM (2000) Delavirdine: a review of its use in HIV infection. Drugs 60:1411–1444
26. Gilden D (1996) Delavirdine/protease inhibitor interactions. GMHC Treat Issues 10:11–12
27. Best BM, Goicoechea M (2008) Efavirenz - still first-line king? Expert Opin Drug Metab Toxicol 4:965–972. doi:10.1517/17425255.4.7.965
28. Dailly E, Allavena C, Raffi F, Jolliet P (2005) Pharmacokinetic evidence for the induction of lopinavir metabolism by efavirenz. Br J Clin Pharmacol 60:32–34. doi:10.1111/j.1365-2125.2005.02369.x
29. Pfister M, Labbe L, Lu JF, Hammer SM, Mellors J, Bennett KK, Rosenkranz S, Sheiner LB (2002) Effect of coadministration of

nelfinavir, indinavir, and saquinavir on the pharmacokinetics of amprenavir. Clin Pharmacol Ther 72:133–141. doi:10.1067/mcp.2002.126183
30. Pham PA, Hendrix CW, Barditch-Crovo P, Parsons T, Khan W, Parish M, Radebaugh C, Carson KA, Pakes GE, Qaqish R, Flexner C (2007) Amprenavir and lopinavir pharmacokinetics following coadministration of amprenavir or fosamprenavir with lopinavir/ritonavir, with or without efavirenz. Antivir Ther 12:963–969
31. Martinez E, Nelson M (2010) Simplification of antiretroviral therapy with etravirine. AIDS Rev 12:52–59
32. Tseng A, MacArthur RD (2010) Profile of etravirine for the treatment of hiv infection. Ther Clin Risk Manag 6:49–58. doi:10.2147/TCRM.S3128
33. Perez VE, Sanchez-Parra C, Villar SS (2009) Etravirine drug interactions. Enferm Infecc Microbiol Clín 27(Suppl 2):27–31. doi:10.1016/S0213-005X(09)73216-1
34. Peytavin G (2008) clinical pharmacokinetic of maraviroc. Méd Mal Infect 38(Suppl 1):S12–S16. doi:10.1016/S0399-077X(08)70539-0
35. Abel S, Jenkins TM, Whitlock LA, Ridgway CE, Muirhead GJ (2008) Effects of cyp3a4 inducers with and without cyp3a4 inhibitors on the pharmacokinetics of maraviroc in healthy volunteers. Br J Clin Pharmacol 65(Suppl 1):38–46. doi:10.1111/j.1365-2125.2008.03134.x
36. Abel S, Russell D, Taylor-Worth RJ, Ridgway CE, Muirhead GJ (2008) Effects of cyp3a4 inhibitors on the pharmacokinetics of maraviroc in healthy volunteers. Br J Clin Pharmacol 65(Suppl 1):27–37. doi:10.1111/j.1365-2125.2008.03133.x